Journal of Hazardous Materials 335 (2017) 56–65

Contents lists available at ScienceDirect

Journal of Hazardous Materials

journal homepage: www.elsevier.com/locate/jhazmat

Insights into key factors controlling GO stability in natural surface waters

Yang Gao[a,b], Xuemei Ren[a,*], Xiaoli Tan[a], Tasawar Hayat[c,d], Ahmed Alsaedi[c], Changlun Chen[a,b,c,*]

[a] Institute of Plasma Physics, Chinese Academy of Sciences, P.O. Box 1126, Hefei 230031, PR China
[b] Collaborative Innovation Center of Radiation Medicine of Jiangsu Higher Education Institutions, Soochow University, Suzhou 215123, PR China
[c] NAAM Research Group, King Abdulaziz University, Jeddah 21589, Saudi Arabia
[d] Department of Mathematics, Quaid-I-Azam University, Islamabad 44000, Pakistan

HIGHLIGHTS

- How each component of surface water affecting on GO stability was investigated.
- Although anion affect cation threshold, GO stability depends on cation type dominantly.
- Monovalent and bivalent cations induce GO aggregation by different mechanisms.
- GO aggregates induced by Na^+, K^+, Ca^{2+} and Al^{3+} are hard to re-disperse.
- GO aggregation in surface water is controlled by its binding with Mg^{2+} and Ca^{2+}.

ARTICLE INFO

Article history:
Received 21 January 2017
Received in revised form 5 April 2017
Accepted 7 April 2017
Available online 11 April 2017

Keywords:
Natural surface waters
GO
Aggregation mechanism
Sedimentation

ABSTRACT

The effects of pH, cations (Na^+, K^+, Mg^{2+}, Ca^{2+} and Al^{3+}), and anions (Cl^-, HCO_3^-, HPO_4^{2-} and SO_4^{2-}) on graphene oxide (GO) stability were investigated to address the current limitations in the knowledge regarding the stability of GO in natural surface water and its underlying mechanism. The threshold values of cations that destabilize GO were obtained and affected by both pH and anions. By employing elemental mapping and studying the effects of polyacrylic acid (PAA) on GO sedimentation and the re-dispersion of GO aggregates, we find that the GO aggregates induced by Na^+ and K^+ via electric double layer suppression and by Ca^{2+} and Al^{3+} via strong complxing are difficult to re-disperse completely. Specifically, more PAA is needed to re-disperse GO aggregates than to stabilize GO, which suggests that after GO binds with heavy metal ions. It is less likely to be transported over a long distance even in natural water that are rich in natural organic matter. Finally, we find that the key factor controlling GO sedimentation in natural surface waters is its binding with Mg^{2+} and Ca^{2+}. This study is expected to provide critical knowledge to more accurately predict the fate of GO in natural surface aquatic environments.

1. Introduction

Since it was discovered by Geim and Novoselov [1,2], the unique structure and outstanding characteristics of graphene oxide (GO) greatly have increased its commercial synthesis and application [3,4]. The worldwide application of GO will inevitably bring problems related to environmental pollution during its synthesis, transport, use and disposal [5,6]. With it eventually ending up in the environment, GO's potential risk to the environment, human health and ecosystem must to be studied thoroughly to assess its environmental fate [7–9].

The colloidal property and stability of GO related to solution chemistry in the aquatic system have attracted researchers' interest [10–13]. It has been found that pH, salt type, ionic strength and natural organic matter greatly affect the aggregation process of GO. GO is stable at pH values between 4.0 and 10.0. High ionic strength could facilitate GO destabilization [10,13,14]. The tendency of GO to agglomerate decreases in the order of $Ca^{2+} > Mg^{2+} > K^+ \approx Na^+$. The presence of anions such as HPO_4^{2-} can slightly improve GO stability

* Corresponding authors at: Institute of Plasma Physics, Chinese Academy of Sciences, P.O. Box 1126, Hefei 230031, PR China.
E-mail addresses: renxm1985@163.com (X. Ren), clchen@ipp.ac.cn (C. Chen).

http://dx.doi.org/10.1016/j.jhazmat.2017.04.027
0304-3894/

at low ionic strengths. However, the increase of cation concentration has a more prominent influence on GO's colloidal properties than does the increase of anion concentration [15]. The stability of GO improved markedly in the presence of natural organic matter (NOM) due to steric and electronic repulsion [16]. However, most previous studies were conducted under idealized conditions. There is still a great knowledge gap between the simplified model results and the actual behaviors of GO in natural waters, because surface water environments include a complex mixture of ions (e.g., Na^+, K^+, Mg^{2+}, Ca^{2+}, Cl^-, HCO_3^- and SO_4^{2-}) and NOMs, which may have a complicated impact on GO stability.

To address the current limitations in knowledge regarding the stability of GO in natural surface waters and its underlying mechanism, we thoroughly investigated the stability and sedimentation kinetics of GO under different aquatic chemistry conditions, including pH as well as the type, valence and concentration of cations (i.e., Na^+, K^+, Mg^{2+}, Ca^{2+} and Al^{3+}) and anions (i.e., Cl^-, HCO_3^-, HPO_4^{2-} and SO_4^{2-}). In particular, the sedimentation kinetics of GO in the mixed Na–Mg systems, and the effect of polyacrylic acid (PAA, a surrogate of natural organic matter) on both GO sediment and the re–dispersion of GO aggregates were assessed. In addition to the well–controlled aquatic solution chemistry studies, we studied the sedimentation kinetics of GO in three natural surface waters collected from Dongpu Lake, Nanfei River, and Chaohu Lake (Hefei city, China). Through this work, we want to identify potentially favorable and unfavorable conditions for GO sedimentation in natural surface waters and to find its critical controlling factor.

2. Materials and methods

2.1. Materials

All of the chemicals used in these experiments were of analytical grade. The natural flake graphite purchased from the Co. Ltd. of TianHe Graphite (Qingdao, China) was used to synthesize GO using the modified Hummers method [17]. FT-IR measurement was obtained from the BrukerEQuinox55 spectrometer. For X-ray photoelectron spectroscopy (XPS) measurement, a VG Scientific ESCALAB Mark II spectrometer was used. Milli–Q water (Millipore, Billerica, MA, USA) was used in all experiments except for the characterization of GO's sedimentation kinetics in natural surface waters. The natural surface waters were collected from Dongpu Lake (The biggest reservoir in Hefei city), Nanfei River (the "mother" river of Hefei) and Chaohu Lake (one of the five largest freshwater lakes in China). Fig. 1 shows the geographical location of Dongpu Lake, Nanfei River and Chaohu Lake (from Google Map).

2.2. Batch experiments

The stability and sedimentation kinetics of GO were carried out using a batch technique, in well-controlled aquatic solutions and natural surface waters. The GO stock suspension and the stock solutions of the background electrolytes (NaCl, KCl, $CaCl_2$, $MgCl_2$, $AlCl_3$, $NaHCO_3$, Na_2HPO_4 or Na_2SO_4), PAA and Milli-Q water were added to the glass vials to achieve the desired concentrations of different components. The desired initial pH values of the suspension in each glass vial were adjusted by adding negligible quantities of HCl or NaOH. The batch experiments as a function of the electrolyte concentrations were performed by taking different concentrations of electrolytes at a fixed initial pH (pH = 5.0 ± 0.5 for cations and pH = 8.0 ± 0.5 for anions. These two pH values were chosen, because they are in the pH range of the natural aquatic environment (pH 5.0–9.0), making the volumes of NaOH/HCl used as small as possible or even negligible). The glass vials containing these mixtures were placed on a horizontal shaker and shaken at a constant speed of 150 rpm for 24 h. Subsequently, the glass vials were left undisturbed on a flat surface for 12 h to allow the complete settlement of the large GO aggregates. Finally, the residual GO concentrations (C_e, mg/L) in the supernatant were determined by UV–vis spectrophotometer (UV-2550, PerkinElmer) at a wavelength of 227 nm [15]. All experimental data were averages of triplicate determinations, and the relative errors were approximately 5%.

The zeta potentials and average size of GO were measured using a Nanosizer ZS instrument (Malvern Instrument Co. Worcestershire, UK) at 25 °C. The GO surface morphology after aggregation was examined by transmission electron microscopy (TEM, JEM-2100F). The concentrations (mmol/L) of cations (e.g., Na^+, K^+, Mg^{2+} and Ca^{2+}) in natural surface waters were measured by an inductively coupled plasma emission spectrometer (ICP, Thermo Jarrell Ash Corporation, USA). NOMs in natural waters were measured by total organic carbon analyzer.

3. Results and discussion

3.1. Effect of pH on GO stability in Milli-Q water

The effect of pH on the residual GO concentration in the supernatant (C_e) without the addition of background electrolyte is shown in Fig. 2A. It is obvious in this case that the pH values have no notable effect on the stability of GO from pH 3.0 to 11.0 in this case. However, at pH < 3.0, the values of C_e decrease with decreasing pH values, with the increasing formation of GO aggregates. As the pH value decreases, the carboxyl groups located at the edges of GO are easily protonated; consequently, GO becomes less hydrophilic and forms more aggregates. The zeta potential values of GO in the pH range from 1.5 to 11.0 are shown in Fig. 2B. Note that the zero point charge lies outside the pH range covered by the curve. The zeta potential values of GO decrease with increasing pH values. At pH > 3.0, the values of GO zeta potential are less than −30 mV, resulting in electrostatically stable GO colloids [18]. According to the results of our FT-IR and XPS measurements (Fig. 2D–F), abundant oxygen-containing functional groups exist on the GO nanosheets. Thus it is believed that the ionization of oxygen-containing functional groups leads to increasing the negative charge on the GO nanosheets, thereby generating a stable aqueous suspension due to the strong electrostatic repulsion. Fig. 2C shows the average size of GO as a function of pH value. Generally, the larger average sizes of GO make it easier to aggregate. Therefore, the response of the average size of GO to varying pH value is contrary to that of C_e to varying pH values, with GO average sizes being quite constant (~200 nm) from pH 3.0 to 11.0 and then increasing sharply as pH decreases from 3.0 to 1.5. This increased average sizes (>1000 nm) below pH 3.0 is due to a reduction in the hydrophilicity and negative charge of GO.

The pH value of the natural aquatic environment is usually in range of 5.0–9.0 [10]. Although our results show that there are no notable changes in the surface charge or average size of GO over this range (Fig. 2B and C), in reality, the pH will affect the species of cations, the binding capacity of cations with GO, and the complexation of cations with anions. Thus, pH values are likely to have a potential effect on the fate of GO in natural aquatic environments. Indeed, our results show that the threshold values of NaCl which induces GO aggregation, differ at different pH values, e.g., 5 mmol/L at pH 5.0 and 10 mmol/L at pH 8.0 (in Figs. 3 A and 5 A), similar to the findings of Gudarzi [13]. Thus, the following experiments were carried out at the fixed pH (i.e., pH = 5.0 ± 0.5 for cations and pH = 8.0 ± 0.5 for anions).

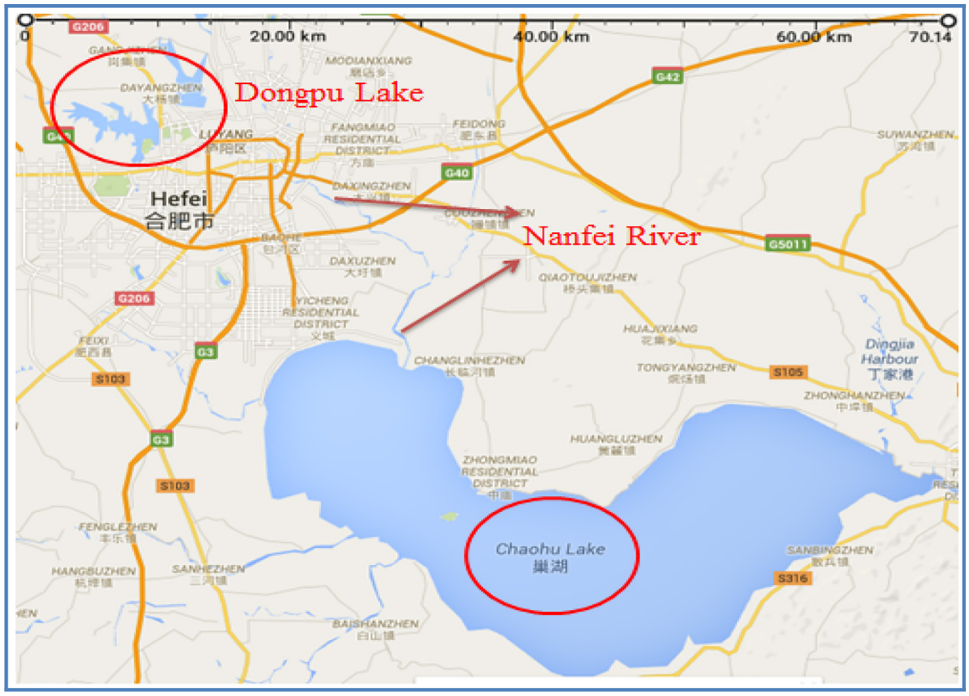

Fig. 1. Geographical location of Dongpu Lake, Nanfei River and Chaohu Lake (from Google Map).

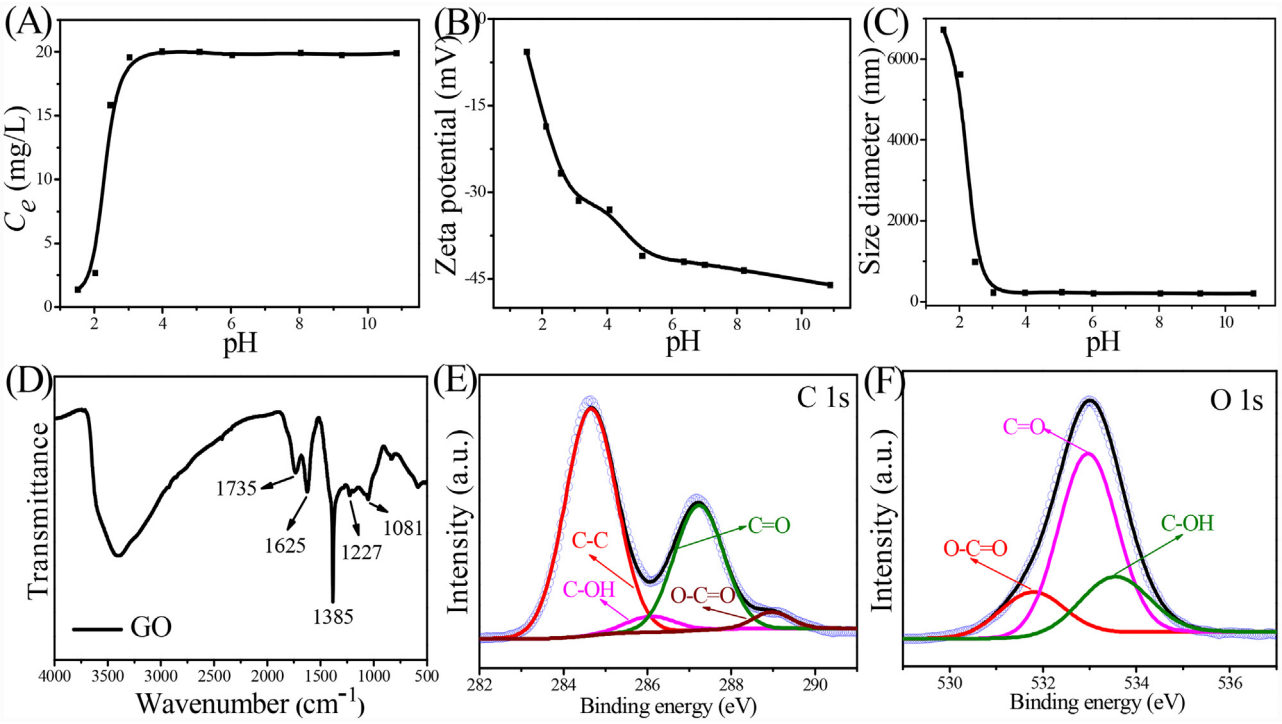

Fig. 2. (A) Concentrations of the residual GO nanosheets in the supernatant as a function of pH, $C_{(GO)initial}$ = 20 mg/L; (B) Zeta potentials of GO as a function of pH; (C) Average size of GO as a function of pH; (D) FT-IR spectra of GO; High-resolution XPS spectra of GO for (E) C 1s peak and (F) O 1s peak.

3.2. *Effect of cation type and concentration on GO stability*

The change of C_e, zeta potential and the size of GO aggregates as a function of the type, valence and concentration of cations (including Na^+, K^+, Mg^{2+}, Ca^{2+} and Al^{3+}), are illustrated in Fig. 3A, B and C, respectively. Fig. 3A shows that the change of C_e obviously depends on not only the ionic strength but also the nature of the dded cation. For all cations, the values of C_e decrease with increasing ionic strength. Note that the value of C_e does not change significantly until the added NaCl concentration reaches a certain threshold value (i.e., 5 mmol/L), which leads to very sharp transitions in this curve as we progressively increase the NaCl concentration. Because Mg^{2+}, Ca^{2+} and Al^{3+} are more efficient in increasing the surface zeta potential of GO (Fig. 3B) and consequently aggregating GO than are K^+ and Na^+ at the same ionic strength, the threshold values observed in Mg–, Ca– and Al–systems are 0.05, 0.05 and

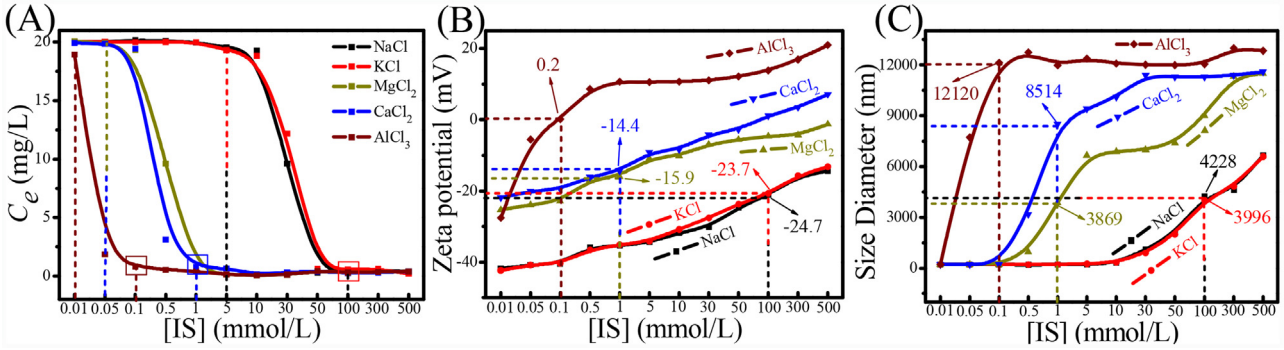

Fig. 3. (A) Concentrations of the residual GO nanosheets in the supernatant as a function of cation type and ionic strength (IS); (B) Zeta potentials of GO as a function of cation type and IS; (C) Average size of GO as a function of cation type and IS. $C_{(GO)initial}$ = 20 mg/L, pH = 5.0 ± 0.5.

0.01 mmol/L, respectively. Similarly, Koh et al. [19] reported that the threshold behavior of carbon nanotubes depended on the added electrolyte type.

In contrast to the response of C_e to the cation concentration, upon addition of various background electrolytes, the zeta potentials of GO display a gradual increasing trend instead of a sharp transition. Based on our results, the GO will settle completely when its overall surface charge increases above a certain threshold value (labeled in Fig. 3B). Fig. 3C shows that the overall average sizes of GO aggregates in the $AlCl_3$ solution are larger than those of GO aggregates in the $CaCl_2$ or $MgCl_2$ solution due to the higher binding capacity of Al^{3+} ions with oxygen-containing functional groups of GO [20–23]. This is further evidenced by the higher quantities of PAA needed to re-disperse GO aggregates in the $AlCl_3$ solution than in the $MgCl_2$ or $CaCl_2$ solution (Fig. 6B). These observations indicate that both the type and concentration of the cation play important roles in the aggregation of GO in aqueous solutions, thus affecting the final fate of GO in natural aquatic environments.

In our case, the destabilizing ability of cations follows the order of $Al^{3+} \gg Ca^{2+} > Mg^{2+} \gg Na^{+} \approx K^{+}$. Based on the Schulze-Hardy rule [24,25], the equivalent cations should induce similar charge screening effects. However, our results show that Ca^{2+} is more efficient in destabilizing GO than Mg^{2+} is, suggesting that the destabilizing capability of metal cation is controlled not only by electric double-layer suppression but also by their adsorption affinity with GO. The latter is determined by the electronegativity and hydration shell thickness of the metal cation [26].

To understand the potential aggregation mechanisms, the microstructures of GO aggregates induced by different cations were characterized. In this study, Na^{+}, Mg^{2+} and Al^{3+} are selected as the typical monovalent, bivalent and trivalent cation, respectively. The concentrations used for Na^{+}, Mg^{2+} and Al^{3+} were set at 50, 1 and 0.1 mmol/L, respectively, levels at which the aggregation of GO initially occurs [27]. The microstructures of GO aggregates induced by Na^{+}, Mg^{2+} and Al^{3+} are presented in Fig. 4 . Selected area electron diffraction (SAED) can be employed to identify the crystalline nature of aggregates from a specific area. Generally, a typical

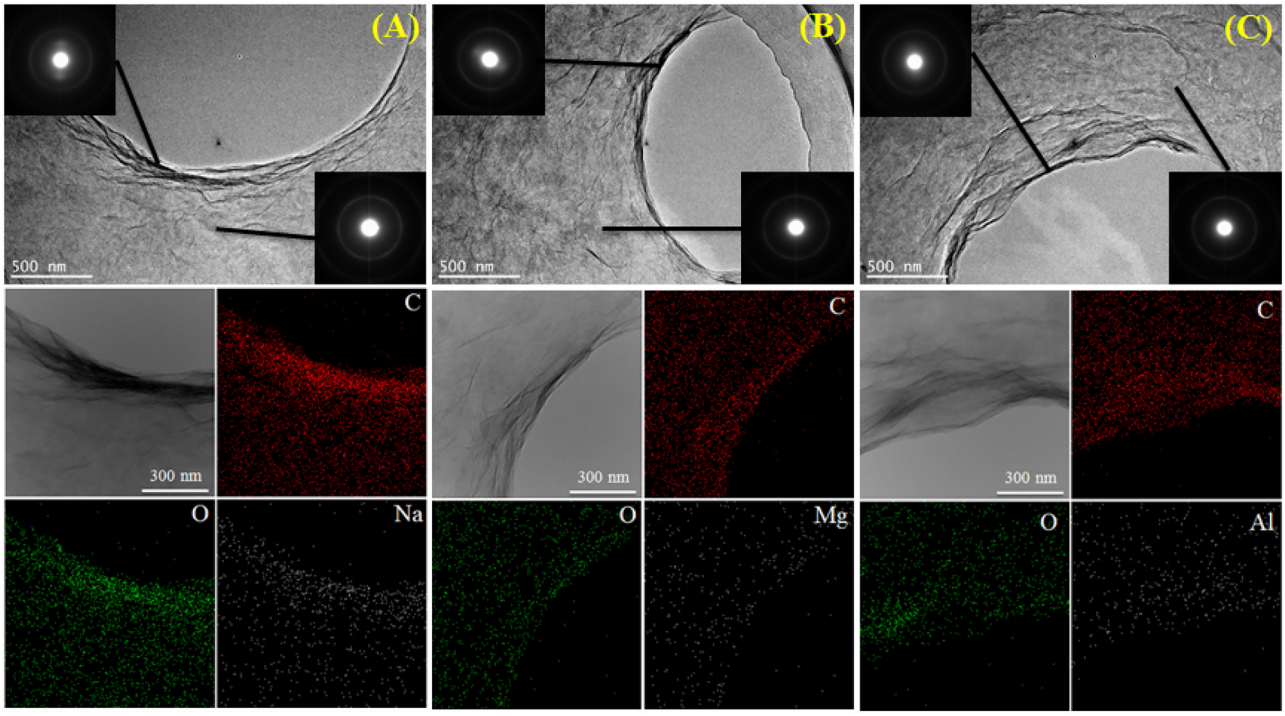

Fig. 4. TEM, selected area electron diffraction (SAED) and element mapping pattern of GO aggregates in the presence of Na^{+}(A), Mg^{2+}(B) or Al^{3+}(C) electrolyte (Na^{+}: 50 mM, Mg^{2+}: 1 mM, Al^{3+}: 0.1 mM and GO: 20 mg/L).

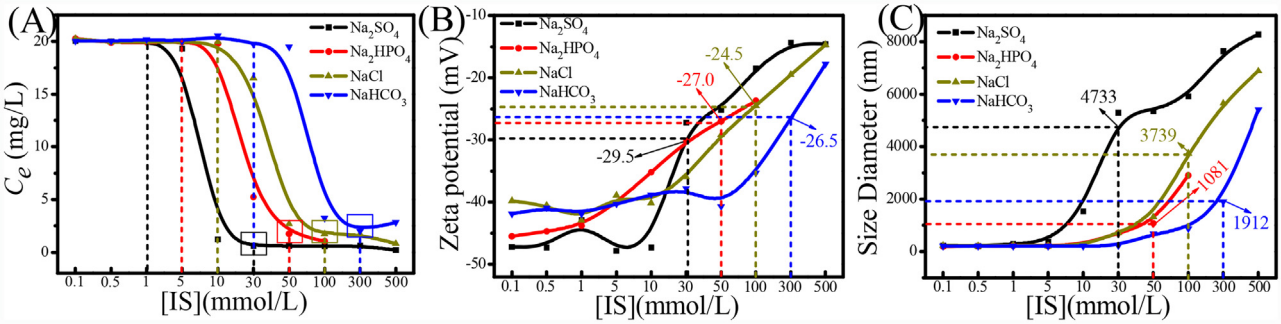

Fig. 5. (A) Concentrations of the residual GO nanosheets in the supernatant as a function of anion type and IS; (B) Zeta potentials of GO as a function of anion type and IS; (C) Average size of GO as a function of anion type and IS. $C_{(GO)initial}$ = 20 mg/L, pH = 8.0 ± 0.5.

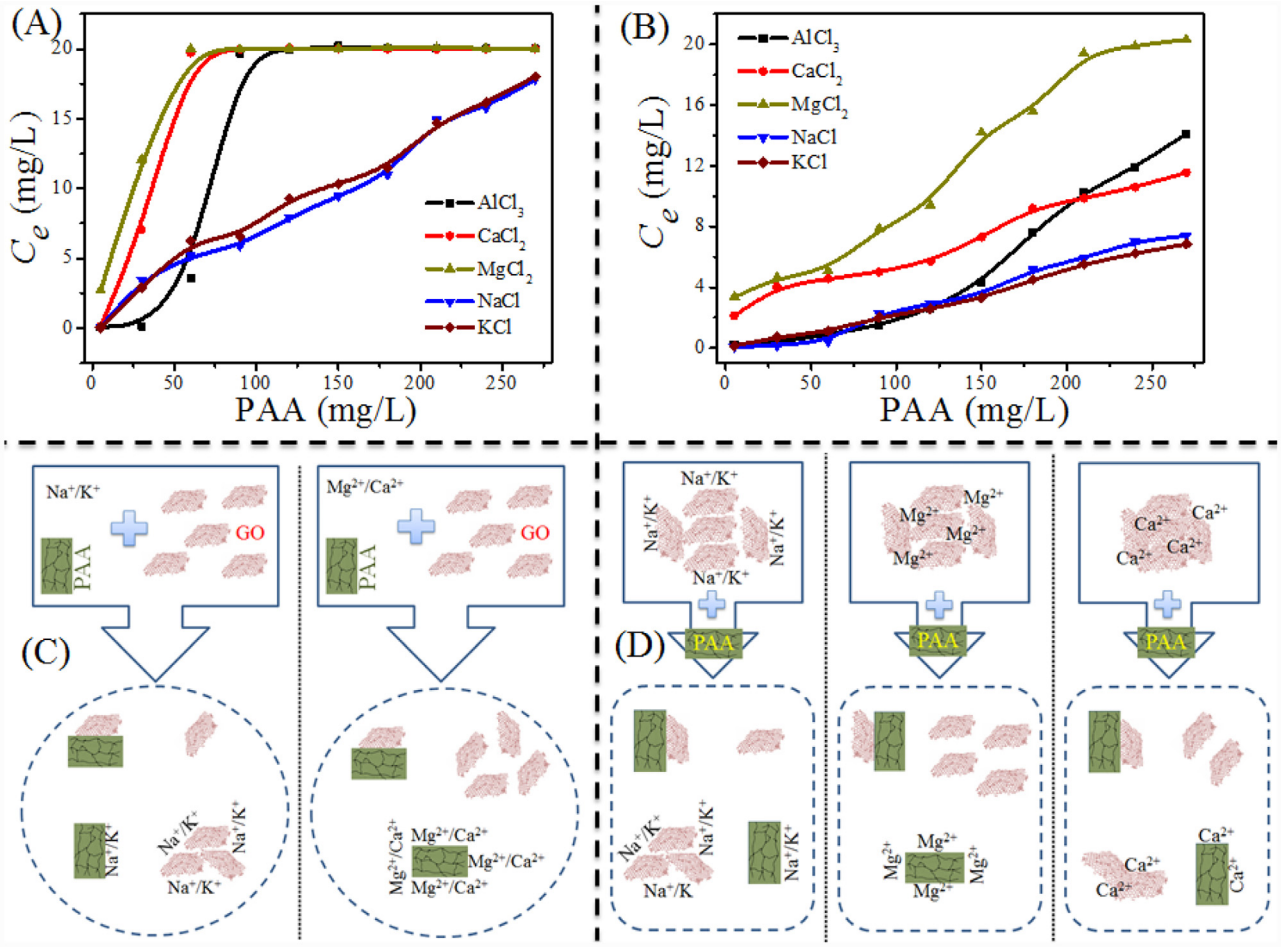

Fig. 6. (A) Effect of PAA concentration on GO sediment: Adding PAA, GO and background electrolyte at the same time; (B) PAA-mediated re-dispersion of GO aggregates: Adding PAA after background electrolyte inducing GO sediment. $C_{(GO)initial}$ = 20 mg/L, pH = 5.0 ± 0.5. The concentrations of cations used to induce GO aggregation are 50 mmol/L NaCl, 50 mmol/L KCl, 1 mmol/L $MgCl_2$, 1 mmol/L $CaCl_2$ and 0.1 mmol/L $AlCl_3$. (C) Schematic diagram of PAA effect on GO sediment; (D) Schematic diagram of PAA-mediated re-dispersion of GO aggregates.

pattern for crystalline materials contains well-defined diffraction spots for single crystal and a set of well-defined diffraction rings for a poly-crystal, whereas those of the amorphous materials contain diffused rings [28]. Fig. 4 only shows the diffused rings, indicating GO aggregates induced by Na^+, Mg^{2+} and Al^{3+} are amorphous.

Furthermore, TEM was used to provide additional evidence of the proposed aggregation mechanism by elemental mapping. From the elemental mapping, one can see that the element positions of C, O and Na/Mg/Al corresponded well to the TEM image. Na is inhomogeneously distributed on the surface of GO, whereas Mg and Al are homogeneously distributed. These TEM images indicate that the aggregation mechanisms of the GO suspension induced by monovalent and multivalent cations are different. Because most of the Na^+ cannot cross the electric double layer, the distribution of Na^+ on GO aggregates is inhomogeneous, and the Na^+ is dominant in inducing the aggregation of GO via electric double layer suppression. In contrast, since Mg^{2+} and Al^{3+} can move across the electric double layer, coordinate with the oxygen containing functional groups, and interact with the basal plane through cation–π binding, the distribution of Mg^{2+} and Al^{3+} on GO aggregates is homogeneous.

Therefore, Mg^{2+} and Al^{3+} dominate inducing the aggregation of GO via complexing.

3.3. Effect of anion type and concentration on GO stability in Milli–Q water

Fig. 5A–C shows the effect of concentrations of Cl^-, HCO_3^-, HPO_4^{2-} and SO_4^{2-} on the C_e, zeta potential and average size of GO, respectively. In these experiments where Na^+ is the counterion, the values of C_e do not change significantly until the added electrolyte concentrations reach a certain threshold value, which leads to sharp transitions in these curves with increasing electrolyte concentrations. Obviously, the added anion type affects this threshold behavior, which roughly follows the order of Na_2SO_4 (1 mmol/L) < Na_2HPO_4 (5 mmol/L) < NaCl (10 mmol/L) < $NaHCO_3$ (30 mmol/L). This is because the anion type affects the potency of Na^+ to destabilize GO, depending on the complexation ability of the anion with Na^+. Overall, the increased Na^+ concentration has more prominent effect on GO stability than does the increased anion concentration; thus, for a certain electrolyte (NaCl, $NaHCO_3$, Na_2HPO_4 or Na_2SO_4), the values of C_e decrease with increasing electrolyte concentration. A mole of either Na_2SO_4 or Na_2HPO_4 has two moles of Na^+ compared with only one mole of Na^+ for NaCl and $NaHCO_3$. Thus, at high concentrations of electrolyte, the presence of Na_2SO_4 and Na_2HPO_4 induces a more pronounced aggregation of GO than that of NaCl and $NaHCO_3$ due to the electric double layer compression caused by Na^+ [11,29]. Finally, the effectiveness of the electrolytes in destabilizing GO follows the order of Na_2SO_4 > Na_2HPO_4 > NaCl > $NaHCO_3$. In contrast to the response of C_e to the varying of the electrolyte concentration, the zeta potentials of GO increase monotonically for all cases (Fig. 5B). The negative charged GO is more likely to attach to Na^+ than to anions, leading to a reduction of the negative surface charge of GO [30,31]. Cl^-, HCO_3^-, HPO_4^{2-} or SO_4^{2-} anions compete with GO for Na^+, so GO exhibits different charge behavior in different electrolytes. Note that at ionic strength (IS) < 5 mmol/L, the surface charges of GO in different electrolyte solutions are in the order of Na_2SO_4 < Na_2HPO_4 < NaCl ≈ $NaHCO_3$. When at IS > 30 mmol/L, the surface charge of GO in different electrolyte solutions are in the order of Na_2SO_4 > Na_2HPO_4 > NaCl > $NaHCO_3$. These observations are attributed to co–ions (i.e., Cl^-, HCO_3^-, HPO_4^{2-} or SO_4^{2-}), below a critical salt concentration, playing an important role in imparting charges onto GO surfaces. In contrast, above a critical salt concentration, electrostatic double layer compression occurs due to the influence of the counterion (Na^+) [32]. Fig. 5C shows the average size of GO as a function of NaCl, $NaHCO_3$, Na_2HPO_4 or Na_2SO_4 concentration. The average size of GO in the Na_2SO_4 solution is larger than that of GO in the NaCl, $NaHCO_3$ or Na_2HPO_4 solution, because GO aggregates most easily in the Na_2SO_4 solution. Although one mole of Na_2HPO_4 contains two moles of Na^+, compared to NaCl, GO in the Na_2HPO_4 solution has a similar average size in the NaCl solution. This is likely attributable to the HPO_4^{2-} preventing the GO particles from getting close to each other due to the stronger electrostatic repulsion and steric hindrance, leading to the destruction of the stacking of GO sheets. This is driven by the $\pi-\pi$ interactions between the graphitic lattices, which can cause a decrease in the size of the GO aggregates [15,33,34].

3.4. Effect of PAA on GO sediment and on re-dispersion of GO aggregates

PAA containing linear CH_2—CH_2 chains and carboxylic groups has properties similar to NOMs. Due to its simple structure, PAA does not disturb the detection of GO by the UV–vis spectrophotometer [15]. Therefore, PAA was used as a NOM surrogate to investigate its effect on GO sediment and the re-dispersion of GO aggregates. Fig. 6A shows the effect of PAA concentration on the sediment process, where GO, background electrolytes and PAA were simultaneously added. We can see that the presence of PAA weakens the effectiveness of cations in inducing the aggregation of GO. The extent of the effect of PAA on different cations follows the order of Mg^{2+} > Ca^{2+} > Al^{3+} > Na^+ ≈ K^+. Specifically, when the concentration of PAA is above a certain threshold value, GO is completely stable in $MgCl_2$, $CaCl_2$ or $AlCl_3$ solution. Obviously, the monovalent and multivalent cations induce the aggregation of GO by different mechanisms, which is consistent with the conclusion drawn by elemental mapping. Based on our results, the presence of PAA has a greater effect on GO sediment via complexing than via electric double layer suppression. Fig. 6C shows a schematic diagram of the PAA effect on GO sediment. In these cases, the stability of GO increases with the PAA concentration due to the following possible reasons. First, PAA competes with GO for binding cations, resulting in weakening the effectiveness of cations in destabilizing GO. Second, PAA with hydrophilic functional groups (—COOH) and a hydrophobic backbone (CH_2—CH_2) can easily be adsorbed onto the GO basal plane through hydrophobic interactions and prevents GO nanosheets from getting close to each other through the steric hindrance effect [35,36]. Meanwhile, the exposed carboxyl groups of PAA make the GO surface more hydrophilic and more negative, which increases the GO stability to a certain extent, depending on the amount and variety of coexisting ions.

Fig. 6B shows the effect of PAA concentration on the re-dispersion of GO aggregates. In this case, the GO and the background electrolyte were added first to induce the zero value of GO concentration in the supernatant (C_e), and different concentrations of PAA were added. Obviously, the addition of PAA can make the bound counterions to desorb from GO, resulting in the re-dispersion of GO aggregates [19]. Fig. 6D shows the schematic diagram of PAA-mediated re-dispersion of GO aggregates. From Fig. 6B, as the concentration of PAA increases, the GO aggregates in the NaCl, KCl, $CaCl_2$ or $AlCl_3$ solution can be partly re-dispersed into solution, while those in the $MgCl_2$ solution can be re-dispersed completely. This suggests that the aggregation processes of GO, which are induced by electric double layer suppression and strong complexing are not fully reversible and that only those induced by weak complexing are fully reversible. In addition, the GO aggregates induced by different mechanisms have different packing structures and a different accessibility of counterions, which has a potential effect on the concentration of PAA needed to re−disperse them [19]. Generally, metal ions with higher binding capacities to GO are more difficult to desorb. Therefore, one can deduce that the binding capacities of multivalent cations to GO increase in the order of Mg^{2+} < Ca^{2+} < Al^{3+}.

Under the same conditions, higher quantities of PAA are needed to re-disperse GO aggregate induced by cations (e.g. 210 mg/L PAA for re-dispersing GO aggregate induced by Mg^{2+} in Fig. 6B) than to stabilize GO in a cation solution (e.g., 60 mg/L PAA for stabilizing GO in 1 mmol/L Mg^{2+} solution in Fig. 6A). This suggests that after serving as a heavy metal ion carrier, GO is less likely to transport over a long distance, even in natural water rich in NOM (e.g., 6.53 ± 0.89% mg/L TOC for Nanfei River in Table 1) [22,37,38]. Accordingly, we deduce that, at higher ph values, greater quantities of PAA are needed to re-disperse GO aggregate, induced by cations. To verify this hypothesis, the effect of PAA on GO sediment in 1 mmol/L $MgCl_2$ and on the re-dispersion of GO aggregates induced by Mg^{2+} were carried out at pH = 7.37 ± 0.1. The results are shown in Fig. S1. One can see that more PAA is needed to re-disperse the GO aggregate induced by Mg^{2+} (>270 mg/L PAA) than to stabilize GO in 1 mmol/L Mg^{2+} solution (60 mg/L PAA) at pH = 7.37 ± 0.1. Therefore, increasing the pH value to 7.37 does not affect the usual tendency. In addition, because a high IS can induce the aggregation

Table 1
Physicochemical properties of the three kinds of natural surface waters.

Water type	pH	TOC (mg/L)	K (mmol/L)	Na (mmol/L)	Mg (mmol/L)	Ca (mmol/L)	Cond (ms/cm)
Dongpu Lake	7.29	4.98 ± 0.14%	0.047	0.27	0.21	0.39	0.16
Nanfei River	7.37	6.53 ± 0.89%	0.28	1.57	0.51	1.23	0.57
Chaohu Lake	8.29	6.16 ± 0.34%	0.37	2.36	0.44	1.06	0.61

of NOM [32], one can deduce that GO is only stable in the natural water containing high concentration of NOM and low IS.

3.5. Cation type effect on sedimentation kinetics of GO in Milli–Q water

The sedimentation rates of GO in aqueous solutions as a function of cation type were presented in Fig. 7A. Cations can somehow compress the electric double layer of GO, neutralize the negative charges of GO, and coordinate with the oxygen containing groups of GO, resulting in the destruction of the stability of GO in solution. Due to the stronger electrostatic attraction between Al^{3+} and GO, and the stronger binding capacity of Al^{3+} with oxygen–containing functional groups of GO,[15] the Al^{3+} is more efficient in increasing the zeta potential values of GO (Fig. 3B). At the same time, the GO aggregates in the $AlCl_3$ solution are larger than those in the $MgCl_2$ or NaCl solution (Fig. 3C). Consequently, the sedimentation kinetic of GO in the $AlCl_3$ solution is the fastest, and no sediment of GO in the NaCl (0.5 mmol/L) solution is observed after 10 h. Specifically, in the $AlCl_3$ solution, a significant and rapid sedimentation is observed at the outset of the experiment for GO, and a slow settling is observed after 6 h. This indicates that when GO comes into contact with Al^{3+}, the GO aggregates with large size form immediately, such that the settlement of GO in the $AlCl_3$ solution may follow two concomitant processes [39]: (1) direct sedimentation of some GO aggregates with large size, and (2) aggregation of the residual GO aggregates with smaller size followed by sedimentation. In contrast, in the $MgCl_2$ solution, a slow settling is observed at the outset of the experiment for GO, and a significant and rapid sedimentation is observed after 6 h. Therefore, when GO comes into contact with Mg^{2+}, the settlement of GO only follows one process: aggregation of the smaller GO aggregates followed by sedimentation. Based on the above statement, the sediment behaviors of GO depends on the cation type.

3.6. Anion type effect on the sedimentation kinetics of GO in Milli–Q water

The sedimentation kinetics of GO in the NaCl, $NaHCO_3$ or Na_2HPO_4 solution over 10 h are shown in Fig. 7B. One can see that the sedimentation kinetics of GO show different trends depending on the anion type. After 6 h, the capacity of electrolytes destabilizes GO following the order of Na_2HPO_4 > NaCl > $NaHCO_3$. With time, the values of C_e change slowly in the $NaHCO_3$ solution, and more obviously in the NaCl and Na_2HPO_4 solutions. The sedimentation rate is slow during the first six hours and then increases sharply, which suggests that when GO comes into contact with NaCl, $NaHCO_3$ or Na_2HPO_4, the settlement of GO follows one process: aggregation of the smaller GO aggregates followed by sedimentation. Because the stronger complexation of HPO_4^{2-} with Na^+ has the potential to weaken the effectiveness of Na^+ in destabilizing GO [40–43], in the first stage, GO is settled more quickly in the NaCl solution than in the Na_2HPO_4 solution. However, with more time, the sedimentation rate of GO in the Na_2HPO_4 solution becomes faster than that in the NaCl solution. This occurs because, as each mole of Na_2HPO_4 contains two moles of Na^+, with time, the higher concentration of Na^+ will induce more pronounced aggregation by electric double layer compression, followed by sedimentation [44,45].

3.7. Sedimentation kinetics of GO at different molar ratios of Na to Mg in mixed cation solution

The sedimentation kinetics of GO in mixed Na–Mg electrolyte systems, with a varying molar ratio of Na^+ to Mg^{2+} but a constant IS are shown in Fig. 7C. One can see that the slowest settling is observed in the solution containing only Na^+, wheares the fastest settling is observed in the solution only containing Mg^{2+}. The values of C_e do not change significantly before the first 6 h in Na–, Mg– and mixed Na–Mg systems. After 6 h, the sedimentation kinetics of GO increase as the molar ratio of Na to Mg decreases. When the molar ratio of Na to Mg is higher than 1, the sedimentation kinetic of GO in mixed Na–Mg system shows a similar trend to that of GO in the Na–system. In contrast, when the molar ratio of Na to Mg is lower than 1, the sedimentation kinetic of GO in the mixed Na–Mg system shows a similar trend to that of GO in the Mg–system. These results suggest that when monovalent and bivalent cations coexist in the system, the sedimentation behavior of GO depends on the molar ratio of the monovalent cation to the bivalent cation. Under our experimental condition, only when the concentration of the bivalent cation in higher than that of the monovalent cation, does the bivalent cation (Mg^{2+}) have more influence in the sediment processes than the monovalent cation (Na^+) [46–48].

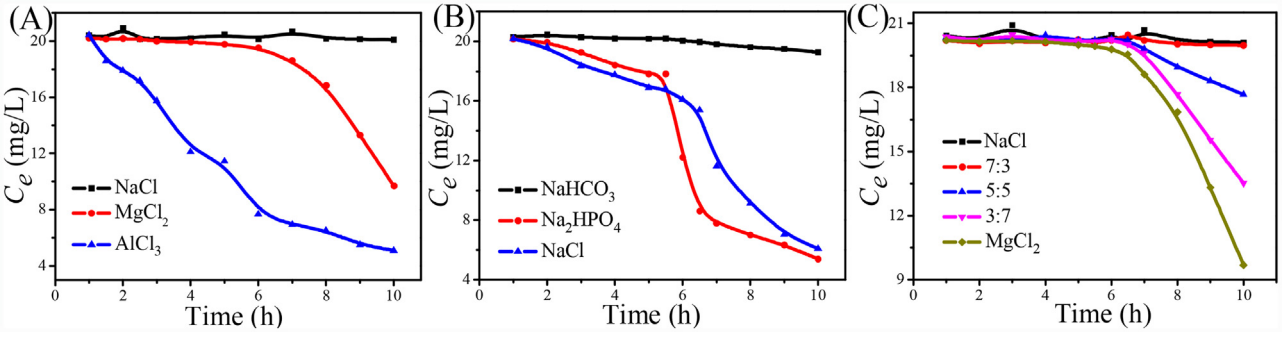

Fig. 7. (A) Sedimentation kinetics of GO nanosheets as a function of cation type (0.5 mmol/L). $C_{(GO)initial}$ = 20 mg/L, pH = 5.0 ± 0.5; (B) Sedimentation kinetics of GO nanosheets as a function of anion type (30 mmol/L). $C_{(GO)initial}$ = 20 mg/L, pH = 8.0 ± 0.5; (C) Sedimentation kinetic of GO nanosheets at different molar ratios of Na to Mg with constant IS (0.5 mmol/L). $C_{(GO)initial}$ = 20 mg/L, pH = 5.0 ± 0.5.

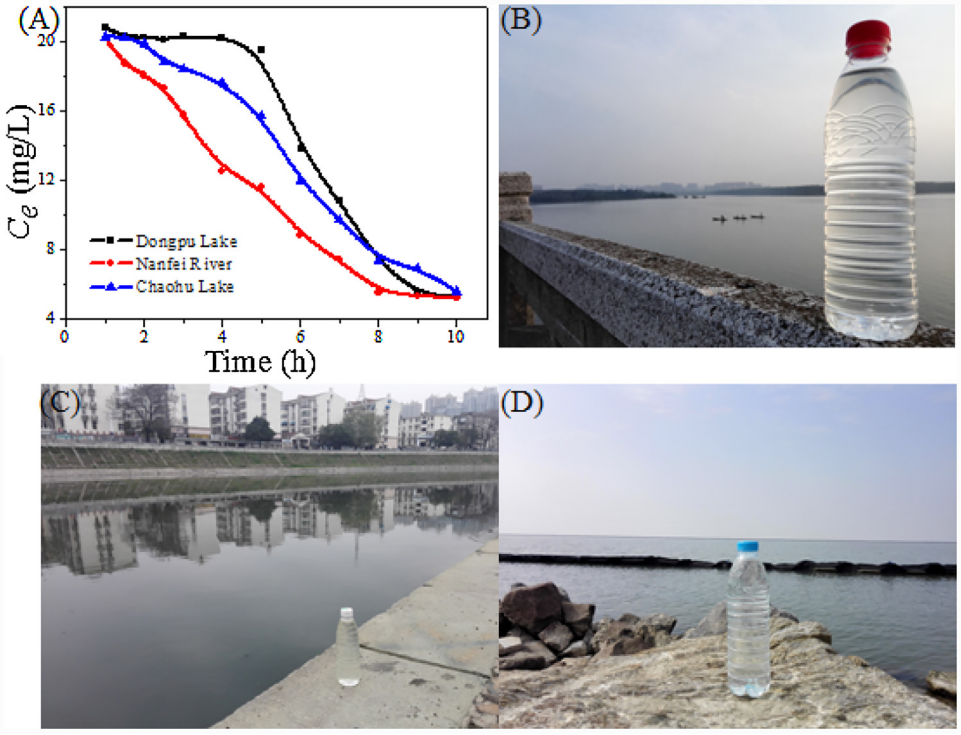

Fig. 8. (A) Sedimentation kinetics of GO nanosheets in the three natural surface waters collected from Dongpu Lake (B), Nanfei River (C), and Chaohu Lake (D).

3.8. Sedimentation kinetics of GO in natural surface waters

The sedimentation kinetics of GO in three natural surface waters collected from Dongpu Lake, Nanfei River and Chaohu Lake in Hefei city are shown in Fig. 8. The tendency of GO to sediment follows the order of Nanfei River > Chaohu Lake > Dongpu Lake. This difference stems from the great difference in the chemical composition of the three natural surface waters [49–53]. The physicochemical properties of the three surface waters are listed in Table 1.

The pH values of Dongpu Lake water, Naifei River water and Chaohu Lake water are 7.29, 7.37, and 8.29 (Table 1), respectively, which are in the range of 3.0–11.0. Over this pH range, we observe no notable changes in the C_e values and the average size of GO (Fig. 1A and C), and the three pH values are close to one another. Thus, it is quite likely that pH has minor effects on sedimentation kinetics of GO in the three natural surface waters without considering electrolyte effect. The water from Dongpu Lake has the lowest concentrations of K^+ (0.047 mmol/L), Na^+ (0.27 mmol/L), Mg^{2+} (0.21 mmol/L) and Ca^{2+} (0.39 mmol/L) (Table 1), and thus has the lowest sedimentation kinetic of GO. The water from Chaohu Lake has more monovalent (K^+: 0.37 mmol/L and Na^+: 2.36 mmol/L) and less bivalent cations (Mg^{2+}: 0.44 mmol/L and Ca^{2+}: 1.06 mmol/L) than does the Nanfei River water (K^+: 0.28 mmol/L and Na^+: 1.57 mmol/L, Mg^{2+}: 0.51 mmol/L and Ca^{2+}: 1.23 mmol/L) (Table 1). Additionally, the Nanfei River crosses the entire city and is more easily polluted by domestic wastewater, so its water probably has much higher amounts of incorporated contaminant. Consequently, the conductivity value of Nanfei River water (0.57 ms/cm) is higher than that of Dongpu Lake water (0.16 ms/cm) (Table 1). Both of these result in GO settling faster in the Nanfei River than in the Chaohu Lake water, which suggests that the multivalent cations play a key role in the process of sedimentation [54,55]. Note that in all natural surface waters, the concentrations of Na^+ and K^+ are lower than their corresponding threshold values (5 mmol/L for Na^+ and 5 mmol/L for K^+), but the concentrations of Mg^{2+} and Ca^{2+} are higher than their corresponding threshold values (0.05 mmol/L for Mg^{2+} and 0.05 mmol/L for Ca^{2+}). This further supports that the aggregation of GO in the three natural surface water can be mainly attributable to the binding of the abundant bivalent cations such as Mg^{2+} and Ca^{2+} with GO [56–58]. Additionally, our results indicate that the NOMs in Dongpu Lake (4.98 ± 0.14% mg/L TOC), Nanfei River (6.53 ± 0.89% mg/L TOC) and Chaohu Lake water (6.16 ± 0.34% mg/L TOC) (Table 1) are not high enough to stabilize the GO. These findings show that once GO is released into the natural surface water rich in multivalent electrolytes, it will be found in the sludge. Undoubtedly, our results clearly demonstrate that, in Dongpu Lake, Nanfei River and Chaohu Lake, it is difficult for GO to remain suspension and to transport over long distances.

4. Conclusions

In this study, we have found that pH will have a minor effect on the fate of GO in the natural aquatic environment without considering the electrolyte effect. Monovalent cations (Na^+ and K^+) induce GO aggregation mainly via electric double layer suppression, which is not reversible. In contrast, multivalent cations (Mg^{2+}, Ca^{2+} and Al^{3+}) induce GO aggregation mainly via their binding with GO, which may be reversible, depending on the binding strength. In a word, the sedimentation behaviors of GO depend on the nature of cation and anion, and on molar ratio of multivalent cation to monovalent cation. When released into the natural surface waters that are rich in abundant bivalent cations, most GO will settle out and end up in the sludge. As a result, GO may be much less stable and mobile in natural aquatic environments (e.g., Dongpu Lake, Nanfei River and Chaohu Lake in Hefei city) than expected. These results provide important insights regarding the dominant factors in the sediment process of GO in the natural surface aquatic environment and would greatly facilitate the evaluation of its environmental impact.

Acknowledgments

Financial supports from the National Natural Science Foundation of China (21477133 and 21377132), Anhui Provincial Natural Science Foundation (1608085QB44), the Jiangsu Provincial Key Laboratory of Radiation Medicine and Protection, the Priority Academic Program Development of Jiangsu Higher Education Institutions are acknowledged.

Appendix A. Supplementary data

Supplementary data associated with this article can be found, in the online version, at http://dx.doi.org/10.1016/j.jhazmat.2017.04.027.

References

[1] A.K. Geim, Graphene: status and prospects, Science 324 (2009) 1530–1534.
[2] K. Novoselov, A. Geim, The rise of graphene, Nat. Mater. 6 (2007) 183–191.
[3] D.R. Dreyer, S. Park, C.W. Bielawski, R.S. Ruoff, The chemistry of graphene oxide, Chem. Soc. Rev. 39 (2010) 228–240.
[4] R.K. Joshi, S. Alwarappan, M. Yoshimura, V. Sahajwalla, Y. Nishin, Graphene oxide: the new membrane material, Appl. Mater. Today 1 (2015) 1–12.
[5] Y. Yang, A.M. Asiri, Z. Tang, D. Du, Y. Lin, Graphene based materials for biomedical applications, Mater. Today 16 (2013) 365–373.
[6] Z. Xiong, C. Liao, X. Wang, A self-assembled macroporous coagulation graphene network with high specific capacitance for supercapacitor applications, J. Mater. Chem. A 2 (2014) 19141–19144.
[7] X. Zhang, W. Hu, J. Li, L. Tao, Y. Wei, A comparative study of cellular uptake and cytotoxicity of multi-walled carbon nanotubes graphene oxide, and nanodiamond, Toxicol. Res. 1 (2012) 62–68.
[8] K.H. Liao, Y.S. Lin, C.W. Macosko, C.L. Haynes, Cytotoxicity of graphene oxide and graphene in human erythrocytes and skin fibroblasts, ACS Appl. Mater. Interfaces 3 (2011) 2607–2615.
[9] O. Akhavan, E. Ghaderi, E. Hashemi, E. Akbari, Dose-dependent effects of nanoscale graphene oxide on reproduction capability of mammals, Carbon 95 (2015) 309–317.
[10] I. Chowdhury, M.C. Duch, N.D. Mansukhani, M.C. Hersam, D. Bouchard, Colloidal properties and stability of graphene oxide nanomaterials in the aquatic environment, Environ. Sci. Technol. 47 (2013) 6288–6296.
[11] I. Chowdhury, N.D. Mansukhani, L.M. Guiney, M.C. Hersam, D. Bouchard, Aggregation and stability of reduced graphene oxide: complex roles of divalent cations, pH, and natural organic matter, Environ. Sci. Technol. 49 (2015) 10886–10893.
[12] L. Wu, L. Liu, B. Gao, R. Mun˜oz-Carpena, M. Zhang, H. Chen, Z. Zhou, H. Wang, Aggregation kinetics of graphene oxides in aqueous solutions: experiments, mechanisms, and modeling, Langmuir 29 (2013) 15174–15181.
[13] M. Moazzami Gudarzi, Colloidal stability of graphene oxide: aggregation in two dimensions, Langmuir 32 (2016) 5058–5068.
[14] Z. Hua, Z. Tang, X. Bai, J. Zhang, L. Yu, H. Cheng, Aggregation and resuspension of graphene oxide in simulated natural surface aquatic environments, Environ. Pollut. 205 (2015) 161–169.
[15] X.M. Ren, J.X. Li, X.L. Tan, W.Q. Shi, C.L. Chen, D.D. Shao, T. Wen, L. Wang, G.X. Zhao, G.P. Sheng, Impact of Al_2O_3 on the aggregation and deposition of graphene oxide, Environ. Sci. Technol. 48 (2014) 5493–5500.
[16] J.D. Lanphere, B. Rogers, C. Luth, C.H. Bolster, S.L. Walker, Stability and transport of graphene oxide nanoparticles in groundwater and surface water, Environ. Eng. Sci. 31 (2014) 350–359.
[17] J. Zhao, F. Liu, Z. Wang, X. Cao, B. Xing, Heteroaggregation of graphene oxide with minerals in aqueous phase, Environ. Sci. Technol. 49 (2015) 2849–2857.
[18] A. Schierz, H. Zänker, Aqueous suspensions of carbon nanotubes: surface oxidation, colloidal stability and uranium sorption, Environ. Pollut. 157 (2009) 1088–1094.
[19] B. Koh, W. Cheng, Mechanisms of carbon nanotube aggregation and the reversion of carbon nanotube aggregates in aqueous medium, Langmuir 30 (2014) 10899–10909.
[20] J. Zhao, Z. Wang, J.C. White, B. Xing, Graphene in the aquatic environment: adsorption, dispersion, toxicity and transformation, Environ. Sci. Technol. 48 (2014) 9995–10009.
[21] H. Mao, W. Chen, S. Laurent, C. Thirifays, C. Burtea, F. Rezaee, M. Mahmoudi, Hard corona composition and cellular toxicities of the graphene sheets, Colloid Surf. B 109 (2013) 212–218.
[22] M.C. Duch, G.S. Budinger, Y.T. Liang, S. Soberanes, D. Urich, S.E. Chiarella, L.A. Campochiaro, A. Gonzalez, N.S. Chandel, M.C. Hersam, Minimizing oxidation and stable nanoscale dispersion improves the biocompatibility of graphene in the lung, Nano Lett. 11 (2011) 5201–5207.
[23] L. Chen, P. Hu, L. Zhang, S. Huang, L. Luo, C. Huang, Toxicity of graphene oxide and multi-walled carbon nanotubes against human cells and zebrafish, Sci. China Chem. 55 (2012) 2209–2216.
[24] J.T.G. Overbeek, The rule of schulze and hardy, Pure Appl. Chem. 52 (1980) 1151–1161.
[25] M. Sano, J. Okamura, S. Shinkai, Colloidal nature of singlewalled carbon nanotubes in electrolyte solution: the schulze-hardy rule, Langmuir 17 (2001) 7172–7173.
[26] K.J. Yang, B.L. Chen, X.Y. Zhu, B.S. Xing, Aggregation, adsorption, and morphological transformation of graphene oxide in aqueous solutions containing different metal cations, Environ. Sci. Technol. 50 (2016) 11066–11075.
[27] K.J. Yang, B.L. Chen, X.M. Zhu, B.S. Xing, Aggregation adsorption, and morphological transformation of graphene oxide in aqueous solutions containing different metal cations, Environ. Sci. Technol. 11 (2015) 11066–11075.
[28] H.C. Xu, C.M. Yang, H.L. Jiang, Aggregation kinetics of inorganic colloids in eutrophic shallow lakes: influence of cyanobacterial extracellular polymeric substances and electrolyte cations, Water Res. 106 (2016) 344–351.
[29] O. Akhavan, E. Ghaderi, Toxicity of graphene and graphene oxide nanowalls against bacteria, ACS Nano 4 (2010) 5731–5736.
[30] A.B. Seabra, A.J. Paula, R. de Lima, O.L. Alves, N. Duran, Nanotoxicity of graphene and graphene oxide, Chem. Res. Toxicol. 27 (2014) 159–168.
[31] X. Li, F. Li, Z. Gao, L. Fang, Toxicology of graphene oxide nanosheets against paecilomyces catenlannulatus, Bul. Environ. Contam. Toxicol. 95 (2015) 25–30.
[32] B. Mukherjee, J.W. Weaver, Aggregation and charge behavior of metallic and nonmetallic nanoparticles in the presence of competing similarly-charged inorganic ions, Environ. Sci. Technol. 44 (2010) 3332–3338.
[33] C.J. Shih, S. Lin, R. Sharma, M.S. Strano, D. Blankschtein, Understanding the pH-dependent behavior of graphene oxide aqueous solutions: a comparative experimental and molecular dynamics simulation study, Langmuir 28 (2011) 235–241.
[34] L.F. Wang, L.L. Wang, X.D. Ye, W.W. Li, X.M. Ren, G.P. Sheng, H.Q. Yu, X.K. Wang, Coagulation kinetics of humic aggregates in mono-and di-valent electrolyte solutions, Environ. Sci. Technol. 47 (2013) 5042–5049.
[35] M. Pham, E.A. Mintz, T.H. Nguyen, Deposition kinetics of bacteriophage MS2 to natural organic matter: role of divalent cations, J. Colloid Interface Sci. 338 (2009) 1–9.
[36] C.L. Chen, X.K. Wang, M. Nagatsu, Europium adsorption on multiwall carbon nanotube/iron oxide magnetic composite in the presence of polyacrylic acid, Environ. Sci. Technol. 43 (2009) 2362–2367.
[37] A.Y. Romanchuk, A.S. Slesarev, S.N. Kalmykov, D.V. Kosynkin, J.M. Tour, Graphene oxide for effective radionuclide removal, Phys. Chem. Chem. Phys. 15 (2013) 2321–2327.
[38] M. Mathesh, J. Liu, N.D. Nam, S.K. Lam, R. Zheng, C.J. Barrow, W. Yang, Facile synthesis of graphene oxide hybrids bridged by copper ions for increased conductivity, J. Mater. Chem. C 1 (2013) 3084–3090.
[39] H. Dong, Y. Xie, G. Zeng, L. Tang, J. Liang, Q. He, F. Zhao, Y. Zeng, Y. Wu, The dual effects of carboxymethyl cellulose on the colloidal stability and toxicity of nanoscale zero-valent iron, Chemosphere 144 (2016) 1682–1689.
[40] S. Park, K.S. Lee, G. Bozoklu, W. Cai, S.T. Nguyen, R.S. Ruoff, Graphene oxide papers modified by divalent ions-enhancing mechanical properties via chemical cross-linking, ACS Nano 2 (2008) 572–578.
[41] T.H. Nguyen, K.L. Chen, Role of divalent cations in plasmid DNA adsorption to natural organic matter-coated silica surface, Environ. Sci. Technol. 41 (2007) 5370–5375.
[42] K.L. Chen, M. Elimelech, Aggregation and deposition kinetics of fullerene (C60) nanoparticles, Langmuir 22 (2006) 10994–11001.
[43] A.R. Petosa, D.P. Jaisi, I.R. Quevedo, M. Elimelech, N. Tufenkji, Aggregation and deposition of engineered nanomaterials in aquatic environments: role of physicochemical interactions, Environ. Sci. Technol. 44 (2010) 6532–6549.
[44] D. Bouchard, W. Zhang, T. Powell, U.S. Rattanaudompol, Aggregation kinetics and transport of single-walled carbon nanotubes at low surfactant concentrations, Environ. Sci. Technol. 46 (2012) 4458–4465.
[45] X. Huangfu, J. Jiang, J. Ma, Y. Liu, J. Yang, Aggregation kinetics of manganese dioxide colloids in aqueous solution: influence of humic substances and biomacromolecules, Environ. Sci. Technol. 47 (2013) 10285–10292.
[46] N.B. Saleh, L.D. Pfefferle, M. Elimelech, Aggregation kinetics of multiwalled carbon nanotubes in aquatic systems: measurements and environmental implications, Environ. Sci. Technol. 42 (2008) 7963–7969.
[47] X.G. Hu, M. Zhou, Q.X. Zhou, Ambient water and visible-light irradiation drive changes in graphene morphology structure, surface chemistry, aggregation, and toxicity, Environ. Sci. Technol. 49 (2015) 3410–3418.
[48] V.C. Sanchez, A. Jachak, R.H. Hurt, A.B. Kane, Biological interactions of graphene-family nanomaterials: an interdisciplinary review, Chem. Res. Toxicol. 25 (2012) 15–34.
[49] K. Rezwan, L.P. Meier, M. Rezwan, J. Voros, M. Textor, L.J. Gauckler, Bovine serum albumin adsorption onto colloidal Al_2O_3 particles: a new model based on zeta potential and UV–vis measurements, Langmuir 20 (2004) 10055–10061.
[50] I. Chowdhury, D.M. Cwiertny, S.L. Walker, Combined factors influencing the aggregation and deposition of nano-TiO_2 in the presence of humic acid and bacteria, Environ. Sci. Technol. 46 (2012) 6968–6976.
[51] L. Feriancikova, S.P. Xu, Deposition and remobilization of graphene oxide within saturated sand packs, J. Hazard. Mater. 235 (2012) 194–200.
[52] L. Liu, B. Gao, L. Wu, V.L. Morales, L.Y. Yang, Z.H. Zhou, H. Wang, Deposition and transport of graphene oxide in saturated and unsaturated porous media, Chem. Eng. J. 229 (2013) 444–449.

[53] A. Philippe, G.E. Schaumann, Interactions of dissolved organic matter with natural and engineered inorganic colloids: a review, Environ. Sci. Technol. 48 (2014) 8946–8962.
[54] W.Z. Teo, M. Pumera, Fate of silver nanoparticles in natural waters; integrative use of conventional and electrochemical analytical techniques, RSC Adv. 4 (2014) 5006–5011.
[55] C.K. Chua, M. Pumera, Light and atmosphere affect the quasi-equilibrium states of graphite oxide and graphene oxide powders, Small 11 (2015) 1266–1272.
[56] E.M. Hotze, T. Phenrat, G.V. Lowry, Nanoparticle aggregation: challenges to understanding transport and reactivity in the environment, J. Environ. Qual. 39 (2010) 1909–1924.
[57] S. Kim, S. Zhou, Y.K. Hu, M. Acik, Y.J. Chabal, C. Berger, W.D. Heer, A. Bongiorno, E. Riedo, Room-temperature metastability of multilayer graphene oxide films, Nat. Mater. 11 (2012) 544–549.
[58] W.Z. Teo, M. Pumera, Graphene oxides: transform ations in natural waters over a period of three months, ChemPlusChem 79 (2014) 844–849.